# Future Design of a New Keratoprosthesis. Physical and Biological Analysis of Polymeric Substrates for Epithelial Cell Growth

Alberto J. Campillo-Fernandez,[†] Silvia Pastor,[‡,||] Marta Abad-Collado,[||] Laurent Bataille,[||] Jose L. Gomez-Ribelles,[†,§] Jose M. Meseguer-Dueñas,[†] Manuel Monleon-Pradas,[†,§] Alberto Artola,[‡,||] Jorge L. Alio,[‡,||] and Jose M. Ruiz-Moreno*[,‡,||]

*Center for Biomaterials, Universidad Politecnica de Valencia, Camino de Vera s/n, 46022 Valencia, Spain, Pathology and Surgery Department, Universidad Miguel Hernandez de Alicante, Ctra. Nacional N-332, 03550 Alicante, Spain, Centro de Investigaciõn Príncipe Felipe, Avenida Autopista del Saler 16, 46013 Valencia, Spain, and Instituto Oftalmolõgico de Alicante (VISSUM), Avenida Denia s/n Edificio Vissum, 03016 Alicante, Spain*

*Received March 15, 2007; Revised Manuscript Received May 4, 2007*

One of the main issues in the development of new biocolonizable materials is to understand the influence of the synthetic material on the biological response in terms of cellular adhesion, proliferation, and differentiation. In this study, we characterized different polymeric materials (with different hydrophobicity/hydrophilicity ratios and electrical charges) using dynamic-mechanical analysis, equilibrium water content, and surface energy. Cell adhesion, viability, morphology, and proliferation studies were conducted with these materials using a conjunctival epithelial cell line (IOBA-NHC). The biological data regarding physicochemical parameters of the materials were also correlated. When conjunctival epithelial cells were grown on poly(ethyl acrylate-*co*-hydroxyethyl acrylate) copolymers, P(EA-*co*-HEA), samples with up to 20% hydrophilic groups on their polymeric chain showed adhesion, viability, and proliferation, although these three factors decreased as the hydrophilic group content increased. The poly(ethyl acrylate-*co*-methacrylic acid) 90/10 copolymer, P(EA-*co*-MAAc) 90/10, showed better results than poly(ethyl acrylate-*co*-hydroxyethyl acrylate) copolymers and were even better than tissue control polystyrene (TCPS). This feature is explained by the presence of electrical charges on the surface of the poly(ethyl acrylate-*co*-methacrylic acid) 90/10 copolymer. The fact that the ionic groups are configured in domains structured in nanophases as happens in this copolymer improves cell adhesion even further.

## Introduction

The cornea is a transparent, nonvascularized tissue with refractive features that depend on the curvature and regularity of its surface. Covering the iris and pupil, the cornea also has a main role protecting the internal ocular structures. Many patients suffering from ocular problems because of corneal opacification can be treated successfully by corneal grafting, also known as penetrating keratoplasty. Some of these patients are considered at high risk of graft failure because of repeated immunological rejections or because of the severity of the corneal affection. In these cases, keratoprosthesis could be an option to allow these patients a correct visual recovery.[1] Postoperative complications such as extrusion, melting, or endophthalmitis are still frequent and severe enough to limit the use of keratoprosthesis and to try to find better materials to reduce these complications. The engineering of the cornea lens using tissue engineering techniques has also been proposed,[2−5] although the reconstruction of the highly ordered cells and extracellular matrix that gives to the cornea its transparency and particular optical properties would appear to be still beyond reach.

One of the main aims related to the design of a good keratoprosthesis is to find new, better biocolonizable materials to improve the biointegration of the prosthesis in the eye. These new biomaterials should also minimize the risks of rejection. The design of the keratoprosthesis includes a central part, optics made from an optical and flexible material of similar composition as the peripheric part, which should allow colonization to occur only on the anterior surface but not on the posterior one, since this would result in corneal opacification.[6] Keratoprostheses should be implanted in a similar way to penetrating keratoplasty.[1,7]

Different research groups have synthesized materials to develop an artificial keratoprosthesis (Legais and co-workers,[8−13] Chirila and co-workers,[14−18] Trinkaus-Randall and co-workers,[19−23] and von Fischern et al.[24]). Clinical trials using Chirila keratoprosthesis (polyhydroxyethyl methacrylate hydrogel) showed that thick synthetic biocompatible structures can be maintained in the cornea without risk of extrusion, helped by fibroblast ingrowth onto the peripheral portion.[25] It has been commonly accepted that one of the main causes of keratoprosthesis failure is the lack of a protective coating layer of epithelial cells.[6,26] Cellular adhesion to polymeric substrates depends on the physical and chemical characteristics of the biomaterial surface. Roughness, stiffness, water content in equilibrium, surface energy, hydrophilicity, and presence of electrical charges, protein absorption, and specific anchoring sites have been shown to influence cellular adhesion, proliferation, and viability.

* To whom correspondence should be addressed. Phone: +34 902 333 344 ext 2403. Fax: +34 965 160 468. E-mail: rdioa@vissum.com.
[†] Universidad Politecnica de Valencia.
[‡] Universidad Miguel Hernandez de Alicante.
[§] Centro de Investigación Príncipe Felipe.
[||] Instituto Oftalmológico de Alicante.

10.1021/bm0703012 CCC: $37.00 
Published on Web 06/27/2007

**Table 1.** Sample Composition, Equilibrium Water Content, and Surface Tension Measured after Liquid Water Immersion at 37 °C for 48 h

| sample | composition | EWC (×100) | $\gamma_p$ (mN/m) | $\gamma_d$ (mN/m) | $\gamma_s$ (mN/m) |
|---|---|---|---|---|---|
| BH000 | PEA | 1.7 ± 0.4 | 0.1 ± 2.3 | 31.0 ± 1.6 | 31 ± 4 |
| BH010 | P(EA-*co*-HEA) 90/10 wt % | 2.3 ± 0.3 | 1 ± 3 | 26 ± 3 | 28 ± 6 |
| BH020 | P(EA-*co*-HEA) 80/20 wt % | 2.8 ± 0. 3 | 1 ± 11 | 29 ± 5 | 30 ± 15 |
| BH030 | P(EA-*co*-HEA) 70/30 wt % | 7.6 ± 0.9 | 1 ± 4 | 31 ± 4 | 32 ± 8 |
| BH050 | P(EA-*co*-HEA) 50/50 wt % | 18.2 ± 1.7 | 3 ± 9 | 33 ± 5 | 36 ± 14 |
| BH070 | P(EA-*co*-HEA) 30/70 wt % | 40.6 ± 1.3 | 3 ± 6 | 35 ± 5 | 37 ± 11 |
| BH100 | PHEA | 134 ± 5 | 19 ± 7 | 27 ± 5 | 46 ± 12 |
| BM010 | P(EA-*co*-MAAc) 90/10 wt % | 3.3 ± 0.1 | 5 ± 3 | 29 ± 3 | 34 ± 6 |
| TCPS | polystyrene | | | | |

In this paper, we analyzed cellular parameters such as adhesion, proliferation, and viability of a well-described human conjunctival epithelial cell line (IOBA-NHC)[27] grown on copolymer substrates with different hydrophilic/hydrophobic monomer contents and electrical charges.

The poly(ethyl acrylate-*co*-hydroxyethyl acrylate), P(EA-*co*-HEA), series forms random copolymers because of the similar reactivity of the monomers, whereas the poly(ethyl acrylate-*co*-methacrylic acid), P(EA-*co*-MAAc), series shows a phase separation with randomly distributed nanodomains of the copolymer and PEA aggregates. P(EA-*co*-MAAc) is a polyelectrolyte. Both phase separation and electrical charge distribution on the surface of the substrate immersed in the culture medium can affect the quantity and conformation of the adsorbed proteins and, in turn, affect cell adhesion and proliferation. These materials have been tested recently in monolayer cultures with different cell types such as chondrocytes,[28] embrionary neural explants,[29] and Schawn cells,[30] showing that the effect of the substrate composition on the biological response is not generalized but presents interesting peculiarities depending on the cells cultured.

In our study, we characterized the physical properties of different substrates on the basis of their water content in equilibrium, surface energy, and dynamic-mechanical properties as well as their biological ability to allow cell growth and adhesion to generate a future biocompatible material that could be colonized and that could serve as a support scaffold, part of a keratoprosthesis.

## Materials and Methods

**Substrate Materials.** Ninety-nine percent pure monomers were obtained from Aldrich. Polymer or copolymer networks were synthesized under ultraviolet light at room temperature using 2% of 98% pure ethyleneglycol dimethacrylate (EGDMA) from Aldrich as the crosslinking agent and 0.13% of 98% pure benzoin from Scharlau as the photoinitiator. Low molecular weight molecules were extracted from the polymeric matrix by boiling them in ethanol for 24 h and by vacuum drying them until constant weight. The composition of the different samples is shown in Table 1. Mean roughness of samples was determined by AFM (Nanoscope III, Digital Instruments). Samples, previously dried, were scanned at room temperature. No significant differences were found between the materials observed. Mean value for roughness was 15 ± 3 nm. Absorption of water in equilibrium by the samples was measured by weighting them after immersion in liquid water for 48 h (until reaching constant weight). Dynamic-mechanical experiments, DMA, were carried out at a heating rate of 2 K/min using a Seiko DMS210 instrument at 1 Hz. Contact angle measurements were obtained using a Dataphysics OCA. Samples were hydrated previously in water at room temperature to simulate the state of substrates during culture. Surface tension, $\gamma_s$, calculations of the hydrated samples used the contact angle of glycerol, diiodomethane, and formamide on the substrates. Polar $\gamma_p$ and dispersive $\gamma_d$ components were calculated following the Owens and Wendt method.[31]

**Cells and Growth Conditions.** Normal human conjunctival (IOBA-NHC) cells spontaneously immortalized and on passage 73 were cultured on different polymeric substrates previously sterilized with $\gamma$ radiation, 25 kGy (Aragogamma, SA), with an approximate diameter of 3 mm and 1−1.5 mm in thickness. Cells were plated onto the different biomaterials on 96 well plates and were washed overnight with sterile 1× DPBS (Sigma); tissue culture treated polystyrene (TCPS) well plates were used as the positive control for cell growth. The following day, PBS was removed from wells and the substrates were equilibrated with complete culture medium (cDMEM/F12) containing 2.5 $\mu$g/mL fungizone, 5000 U/mL penicillin/streptomycin, 2 ng/mL mouse epithelial growth factor (EGF), 1 $\mu$g/mL bovine pancreas insulin, 0.1 $\mu$g/mL cholera toxin, 5 $\mu$g/mL hydrocortisone, and 10% heat-inactivated fetal bovine serum for at least 8 h. After this time, the medium was removed and the cells were seeded at a density of $5 \times 10^3$ cells/mL in 10 $\mu$L of complete DMEM/F12 as described above. Cells were left for decantation for at least 2 h after which 200 $\mu$L/well of culture medium was gently added. Incubation was performed at 37 °C in a 5% $CO_2$ incubator. The medium was changed every 2−3 days.

**Cellular Adhesion and Viability.** For cell adhesion analysis at the specified time points, cells were gently washed two times with 200 $\mu$L of 1× DPBS to remove the culture medium, and then the substrates were moved into a new 96 well plate, were trypsinized using 150 $\mu$L of 0.25% Trypsin with 1 mM EDTA per well, and were incubated for 90 s at 37 °C in a 5% $CO_2$ incubator. After this time, trypsin was blocked by adding 150 $\mu$L of cold blocking medium containing DMEM/F12 medium enriched with 10% FBS and 5000 U/mL of the antibiotics penicillin/streptomycin. Triplicate samples were resuspended and pooled into sterile Eppendorf tubes containing an additional 450 $\mu$L of blocking medium. Tubes were centrifuged at 800 rpm for 5 min, were washed once with 1× DPBS, and finally were resuspended with 500 $\mu$L of DPBS. Twofold dilutions were performed with Trypan Blue, and cells were quantitated using a Neubauer chamber. The total number of cells from triplicate wells on each condition was divided by 3 to obtain the number of cells per each support material.

The same culture assays were performed for cell viability analysis at the specified time points. The cells were washed two times with DPBS, and 150 $\mu$L of 0.2% Trypan Blue diluted in PBS was added to the wells which were then incubated at room temperature for 10 min. After this period, the vital colorant was removed, and cells were washed two times with DPBS. Cells were observed under an inverted optical microscope Zeiss Axiovert 200 and were photographed.

**Cell Morphology. Hematoxylin and Eosin Staining (H&E).** For the morphology evaluation, H&E staining was performed on fixed biomaterials cultured as above. Briefly, the colonized biomaterials were washed two times with DPBS, were fixed with 4% paraformaldehyde (PFA) for 20 min at room temperature, and were washed two times with DPBS and two times with distilled water ($dH_2O$). All washes were 5 min per wash. After this, the biomaterials were submerged into Mayer's Hematoxylin (Merk) for 3 min and then were washed with $dH_2O$ for 5 min. Next, the samples were washed for 2 min in 80% ethanol and for 5 min with Eosin Y (Electron Microscopy Sciences).

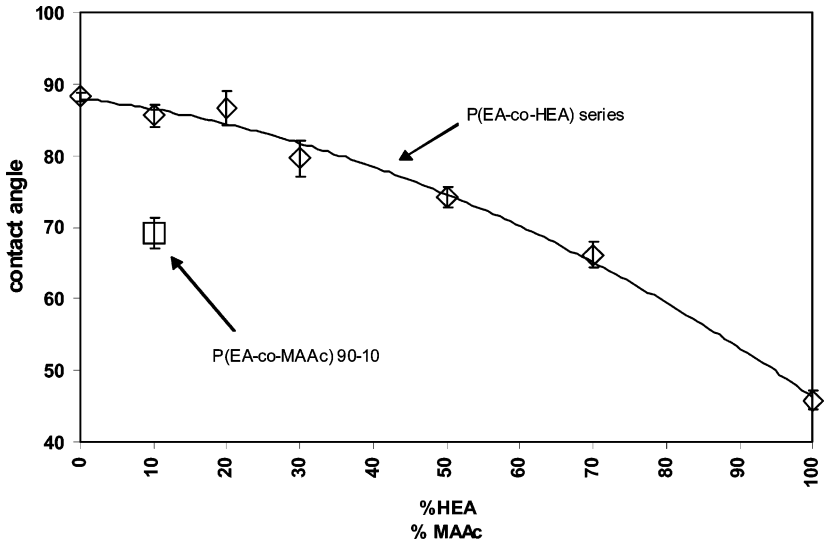


**Figure 1.** Contact angle measurements for a formamide drop on P(EA-*co*-HEA) and P(EA-*co*-MAAc) copolymers.

Finally, the samples were dehydrated in four steps, 5 min in 96% ethanol, 5 min in 100% ethanol, and the two last steps in Xilol (Panreac), 5 min each. The substrate materials were then mounted onto microscope slides with a special mounting medium (Electron Microscopy Sciences) and were observed using an optical microscope Zeiss Axiovert 200.

**Analysis of Cell Proliferation.** The DNA-binding CyQUANT NF (Invitrogen, Carlbad, CA) fluorescent proliferation assay kit was used for the analysis of cell proliferation. The cells were grown on the different substrates for 3, 5, and 7 days. Dye binding solution was prepared from stock as described in the datasheet. Briefly, CyQuant NF dye reagent was diluted from stock to 1× working solution in 1× HBSS. At each time point, the growth medium was aspirated from the wells and 100 $\mu$L of binding solution was added and incubated with cells for 30 min at 37 °C. After the incubation time, cells were ready for detection using a Zeiss Axioskop 2 Plus direct microscope with an excitation filter of 450−490 nm.

**Statistical Analysis.** Statistical analysis was performed using the SPSS for Windows (version 11.0.1). The Kruskal−Wallis test was used to compare the mean values of cell numbers for every support biomaterial at each time point. The statistical tests were performed with a 0.05 alpha level for significance.

## Results

**Materials Characterization.** It is well-known that surface properties such as hydrophilicity or surface tension affect cellular adhesion. The equilibrium water content (EWC), the mass of water absorbed per polymer mass unit, of the copolymers is shown in Table 1. Pure PEA matrix absorbs less than 2% of water; hence, it can be considered a hydrophobic material. Water absorption increases uniformly with the hydroxyethyl acrylate content in the P(EA-*co*-HEA) copolymers. The water absorption capacity of P(EA-*co*-MAAc) 90/10 copolymer is slightly higher than that of the P(EA-*co*-HEA) copolymer with the same hydrophilic component content.

We also show the contact angle measurements of the different substrates in the presence of formamide. Contact angle decreases monotonously with increasing HEA content in the P(EA-*co*-HEA) copolymer series. The decrease with respect to PEA homopolymer is more pronounced in the P(EA-*co*-MAAc) copolymer. A single point (the square) corresponding to this copolymer is represented in Figure 1.

Furthermore, the surface energy of the P(EA-*co*-HEA) series, also shown in Table 1, decreases uniformly with the increment of the PEA hydrophobic component. The polar component of the superficial tension, with a high value for the pure hydrophilic PHEA, decreases almost totally in the hydrophobic component. Following the same trend as the equilibrium water content or the contact angle, the polar component of surface energy is much higher in the copolymer containing 10% MAAc than in that containing 10% HEA. The hydrophilic groups affect the biological response not only because they affect the equilibrium water content and the surface tension but also because the distribution of these groups on the surface may be important. Alternating hydrophilic and hydrophobic domains affect protein absorption,[32,33] and this may in turn affect cellular adhesion and proliferation.[28] Something similar may happen with the presence of acid groups that dissociate in the culture medium providing a negative electric charge distribution on the surface of the substrate. That is the reason why nanomorphology of copolymers should be characterized. In the case of the copolymers obtained by free-radical copolymerization in a reactive mixture containing both comonomers, heterogeneity in the monomer distribution may occur as a result of the different reactivity of the two monomers. In some cases, this can lead to copolymer chains that contain long sequences of the same monomeric unit. This homopolymer block can associate forming a nanophase-separated system with alternative domains of different hydrophilicity on the material surface. This was the case of the poly(ethyl acrylate-*co*-hydroxyethyl methacrylate) copolymers, P(EA-*co*-HEMA), a copolymer series similar to the copolymers used in our study.[28] The dynamic-mechanical technique is appropriate to investigate nanophase separation since even very small domains can show their own main relaxation process associated with their glass transition as a peak in the isochronal plot of the loss tangent against temperature with a simultaneous drop of the elastic modulus. As shown in Figure 2, this would appear not to be the case of the P(EA-*co*-HEA) copolymer series since the shape of the loss tangent and the elastic modulus plot is similar in the 50/50 copolymer to the pure homopolymer networks. Nevertheless, a certain phase separation in the swollen state when the copolymer network is immersed in the culture medium cannot be ruled out because of the so-called hydrophobic interaction. In water, there may be a tendency for the hydrophobous segments of the copolymer chain to aggregate to minimize their interaction with the water molecules. This effect is currently under study, and the results will be published elsewhere.

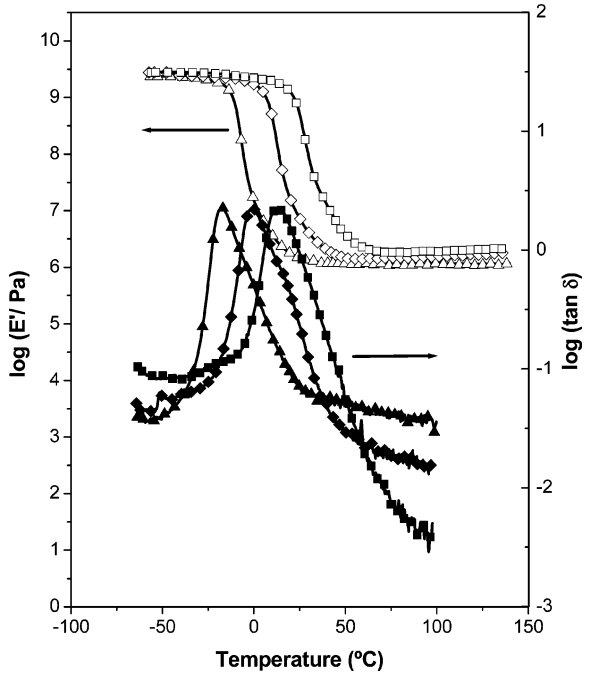


**Figure 2.** Storage modulus (open symbols) and loss tangent (full symbols) of P(EA-*co*-HEA) 50/50 copolymer (◆) compared to that of the PEA (▲) and PHEA (■) homopolymer networks.

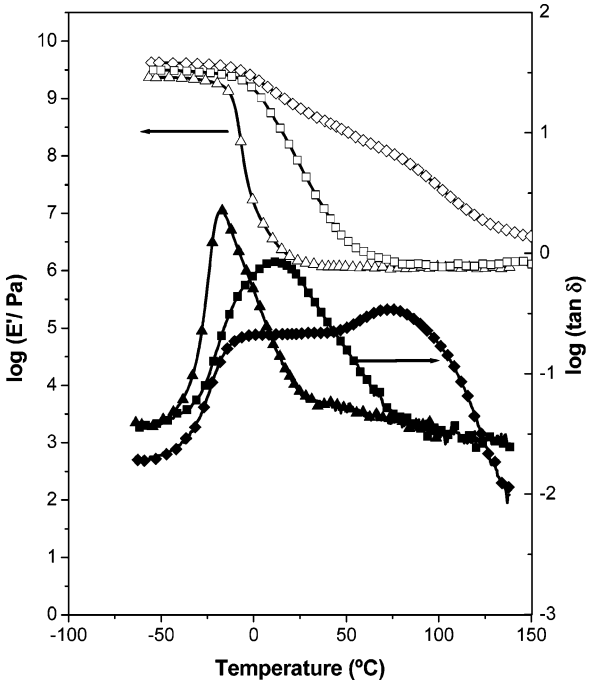


**Figure 3.** Storage modulus (open symbols) and loss tangent (full symbols) of PEA homopolymer (▲) and P(EA-*co*-MAAc) copolymers containing 10% (■) and 20% (◆) MAAc.

In the case of P(EA-*co*-MAAc) copolymers, the situation changes. The shape of the peak of the loss tangent of the copolymer containing 10% MAAc indicates the possible superposition of two peaks. To further clarify this fact, a copolymer containing 20% MAAc was included in the study. As shown in Figure 3, two maxima appear clearly in the loss tangent plot. The low-temperature one, appearing at around 0 °C, can be associated with a phase rich in PEA since the peak appears at the same temperature as in PEA homopolymer (Figure 2). The high-temperature one corresponds to a random copolymer of EA and MAAc. The dynamic-mechanical main relaxation of PMAAc homopolymer network is not shown since it occurs at very high temperatures, after the start of the polymer degradation. Thus, it must be concluded that P(EA-*co*-MAAc) copolymers are phase separated and consist of hydrophobous PEA domains of nanometric dimensions dispersed in a copolymer matrix. P(EA-*co*-MAAc) 80/20 copolymer was not used for cell culture as it lost transparency because of the phase separation.

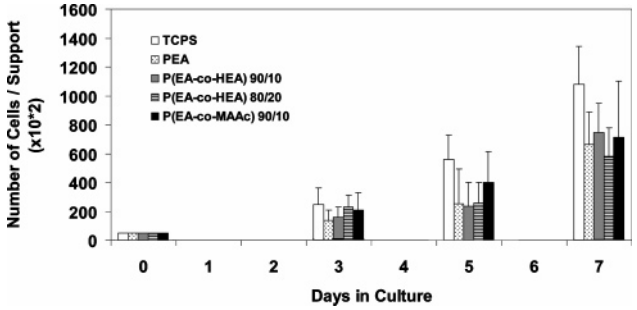


**Figure 4.** Number of cells adhering to the different substrates as a function of time. The data represent a mean of four values for each substrate and time point from four independent experiments, and the error bars represent the standard deviation. The Kruskal−Wallis test was used to compare each biomaterial. No significant differences were observed.

**Cell Culture.** As shown in Figure 4, the number of cells adhering to the different substrates is correlated with the −OH groups present on the surface, that is, the quantity of the hydrophilic component. Thus, for the P(EA-*co*-HEA) series, the more hydrophobic the substrate, the better the adhesion of the IOBA-NHC cells. All substrates with up to 20% of the hydrophilic component showed adhesion whereas IOBA-NHC cell cultures on substrates with more than 20% of hydrophilic component did not show adhesion (data not shown). After one week, cells reached 90% confluence on PEA, P(EA-*co*-HEA) 90/10, P(EA-*co*-HEA) 80/20, P(EA-*co*-MAAc) 90/10, and TCPS, as is shown in Figures 4 and 5. P(EA-*co*-HEA) 90/10 and P(EA-*co*-MAAc) 90/10 showed the best adhesion properties of all hydrophobic biomaterials at day 7 in culture. However, no significant differences were found among the different support biomaterials analyzed at each time point (Kruskal−Wallis test, $p = 0.393$ for day 3, $p = 0.124$ for day 5, $p = 0.175$ for day 7).

Viability observed by Trypan Blue staining showed a majority of living cells with only a few of them stained after 7 days in culture on PEA, P(EA-*co*-HEA) 90/10, P(EA-*co*-HEA) 80/20, P(EA-*co*-MAAc) 90/10, and TCPS (Figure 6).

Cell morphology was analyzed by H&E staining which revealed the characteristic epithelial and polygonal morphology of the IOBA-NHC cells with a large nucleus and numerous intensely stained nucleoli (Figure 7).

Some cultures were kept for over one week, and cells maintained the typical morphology of epithelial cells with an expected death rate because of confluence. None of the materials were toxic for cell growth.

To analyze IOBA-NHC cell proliferation on the different substrates, CyQUANT NF Cell Proliferation Assay Kit containing a fluorescence DNA-binding dye allowed us to get a photographic registry through a fluorescence microscope. The follow-up revealed a high level of proliferation increasing from day 0 to 7 (Figure 8).

## Discussion

The literature has demonstrated that the impact on substrate surface cell adhesion of the presence of hydrophilic groups

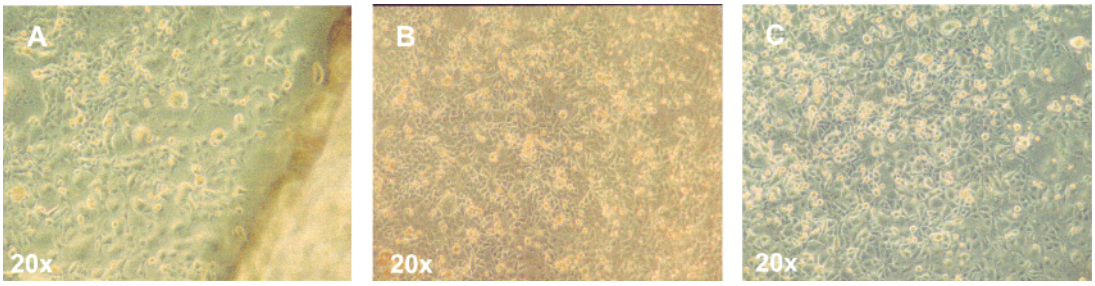


**Figure 5.** IOBA-NHC cells after 7 days of culture on (A) PEA, (B) P(EA-*co*-MAAc) 90/10, and (C) TCPS. Images show a 20× lens magnification with a Zeiss Axiovert 200 inverted microscope, as indicated.

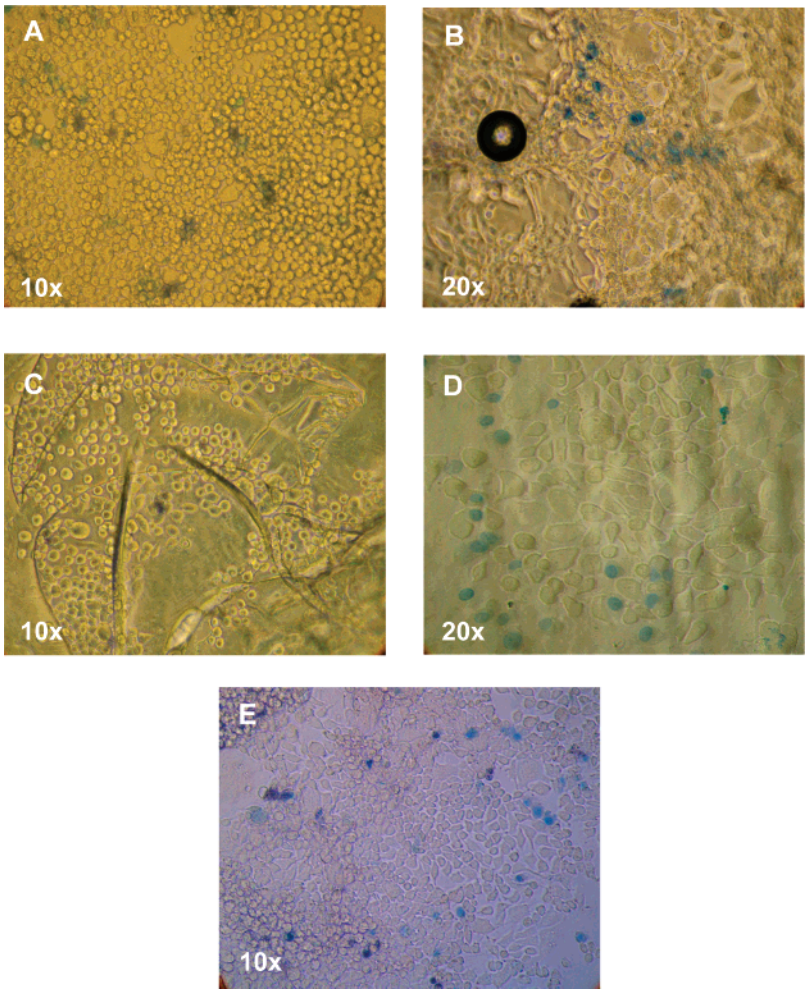


**Figure 6.** Trypan Blue staining of IOBA-NHC cells on different substrates: (A) PEA, (B) P(EA-*co*-PHEA) 90/10, (C) P(EA-*co*-HEA) 80/20, (D) P(EA-*co*-MAAc) 90/10, and (E) control TCPS. Cells were viable for up to one week until they reached confluence. Images show a 10× or a 20× lens magnification with a Zeiss Axiovert 200 inverted microscope, as indicated.

depends highly on the surface distribution of these groups and on the cell type. While cell adhesion is not possible on hydrophilic polymers like poly(hydroxyethyl methacrylate) (PHEMA), with fibroblasts and other cell lines, cellular anchoring is feasible with hydrophobic polymers like poly(methyl methacrylate) (PMMA) or poly(ethyl methacrylate) (PEMA).[35−39]

In the present study with epithelial conjunctival cells (*IOBA-NHC*), we have shown that the higher the hydrophilic component content in the P(EA-*co*-HEA) series, the lower the cellular adhesion. P(EA-*co*-HEA) 90/10 and P(EA-*co*-MAAc) 90/10 showed the best adhesion properties, however, no significant differences were observed among all hydrophobic materials analyzed. This is probably due to the high standard deviation obtained since the seeding protocol may vary slightly the final number of cells on each support for each experiment.

These results can be compared with chondrocyte cultures on poly(ethyl methacrylate-*co*-hydroxyethyl acrylate), P(EMA-*co*-HEA), and P(EA-*co*-HEA) substrates, copolymers that do not present phase separation; the higher the HEA content is, the lower the cellular proliferation and adhesion are. Nevertheless, for the poly(ethyl acrylate-*co*-hydroxyethyl methacrylate), P(EA-*co*-HEMA), series where there is a phase separation in the form of alternating hydrophobic and hydrophilic domains, chondrocyte culture parameters are better for the 50−50 ratio copolymer.[28]

In our study, conjunctival epithelial cells show no proliferation after 24 h on PHEA, which is not as evident in other cell types, such as chondrocytes.[28] Conversely, we observe good adhesion on PEA, though not as good as on TCPS.

As observed in Figure 4, 10−20% of HEA present in copolymer allows cell adhesion, although greater amounts do

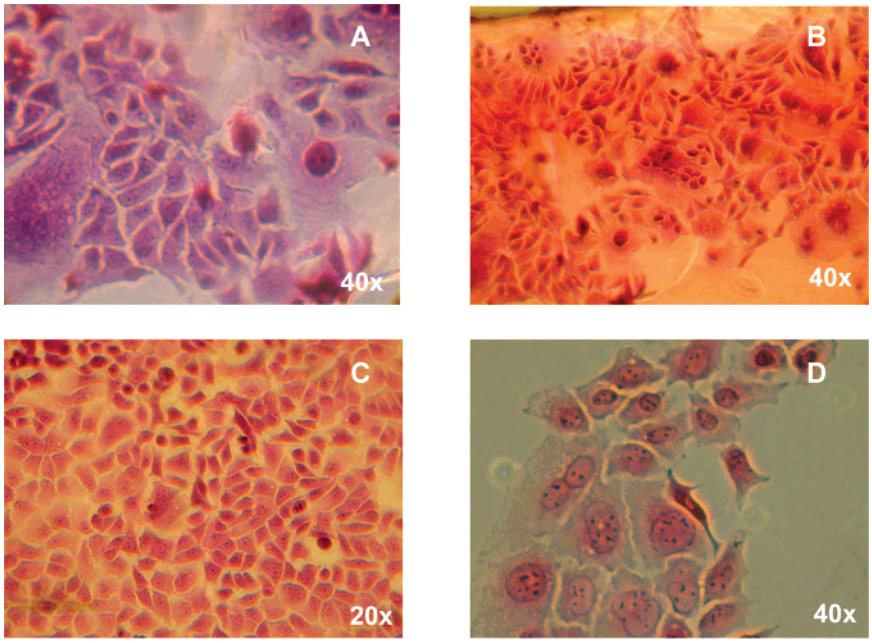


**Figure 7.** Morphology of IOBA-NHC cells grown on different substrates. (A) PEA, (B) P(EA-*co*-HEA) 90/10, (C) P(EA-*co*-MAAc) 90/10, and (D) TCPS after day 7 of culture. Morphology of IOBA-NHC cells on these substrates remained unaltered as in the control. Images show a 20× or a 40× lens magnification with a Zeiss Axiovert 200 inverted microscope, as indicated.

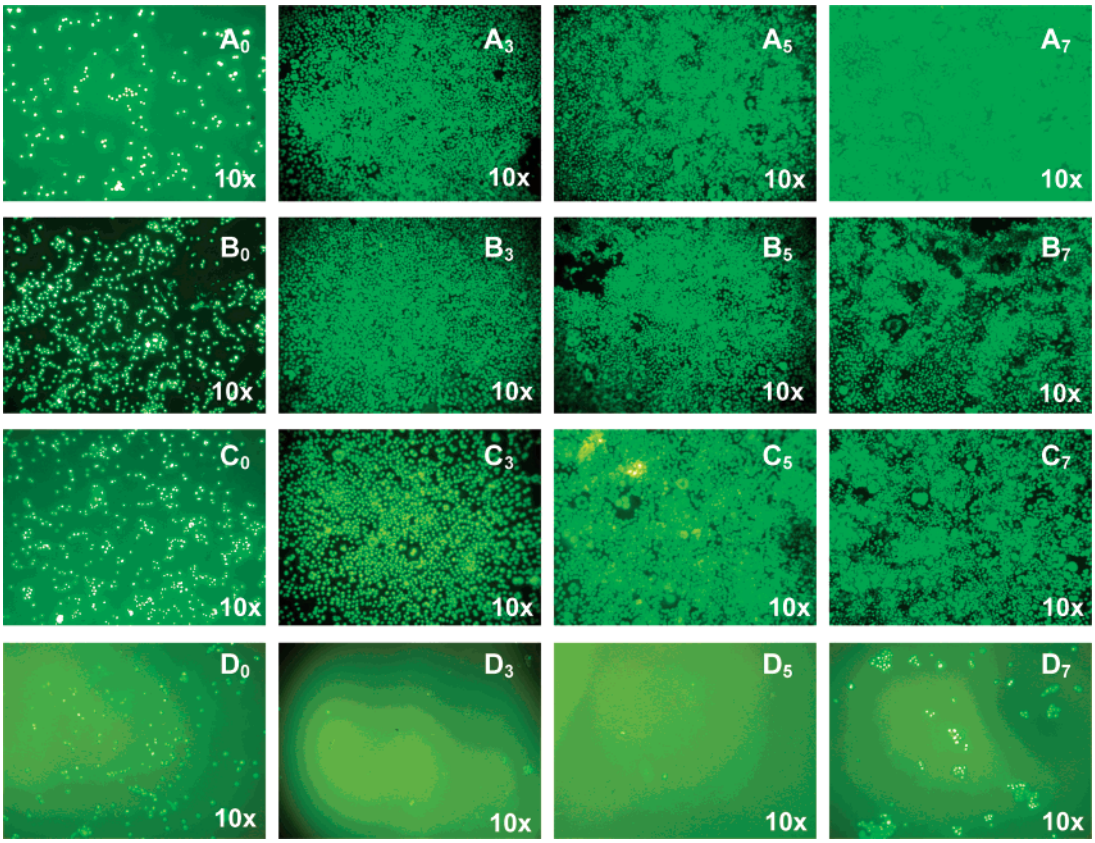


**Figure 8.** Proliferation analysis of IOBA-NHC cells grown on different substrates after 0, 3, 5, and 7 days. (A, B) IOBA-NHC cells growing on PEA and P(EA-*co*-HEA) 90/10, respectively. Cells proliferated optimally throughout the days, and some stratification was observed by day 7. (C) IOBA-NHC cells growing on P(EA-*co*-MAAc) 90/10 showed similar behavior as in PEA and P(EA-*co*-HEA) 90/10 with good adherence and proliferation (D) IOBA-NHC cells growing on PHEA. Very few cells were attached and, hence, low proliferation on the support material was observed. Images show a 10× lens magnification with a Zeiss Axiovert 200 inverted microscope, as indicated.

not show the same behavior. A possible explanation for this could be that serum proteins that do not promote cell adhesion are adsorbed preferentially on the biomaterial or that proteins adsorbed by polymer acquire a conformation with less exposed binding motifs as the hydrophilic content increases. In this sense, once the 20% threshold of HEA is reached, matrixes do not show protein adhesion properties and, hence, cellular adhesion fails.

When MAAc units are added to the polymeric matrix, different results are observed. Although the equilibrium water

content of P(EA-*co*-MAAc) 90−10 is 50% higher than that of P(EA-*co*-HEA) 90−10, it is nonetheless very small, and at the same time, the polar component of surface tension increases dramatically because of the presence of carboxyl groups. Moreover, copolymers with 10% MAAc show phase separation. Besides, because of the acid nature of this copolymer, it dissociates when in contact with water so the surface gets negatively charged favoring cellular adhesion even further.[40] On one hand, the separation of hydrophobous domains can increase cell adhesion in substrates with higher amount of absorbed water[30] in the case of chondrocytes and, on the other hand, distribution of negative charges affects the selection of absorbed proteins and their conformation on the substrate. Probably, both effects contribute to the improved cell adhesion and proliferation, but one cannot be conclusive about which is more important. No correlation between cell adhesion and equilibrium water content and surface energy was found.

According to our data, P(EA-*co*-MAAc) copolymers show better cellular adhesion and proliferation than the TCPS control group. Although there are many studies on cellular adhesion on PMAAc, the combination with PEA, as in our study, is novel to our knowledge. We have also shown that both phase separation and the polyelectrolyte properties of the P(EA-*co*-MAA) copolymer help adhesion and proliferation of conjunctival epithelial cells.

## Conclusions

Optimal cell growth and adhesion of conjunctival epithelial cell cultures have been evaluated on different acrylic substrates with the aim of developing the optical part of a future keratoprosthesis. The P(EA-*co*-HEA) copolymer networks allow epithelial cell growth when containing a maximum of 20% weight of HEA. Higher quantities prevent cellular adhesion and, hence, there was no proliferation observed starting from the first day of culture. The addition of a small amount of methacrylic acid, MAAc, to the hydrophobous PEA component in P(EA-*co*-MAAc) 90−10 copolymer (polyelectrolyte with phase separation) shows the best results, even better than the TCPS control group in some assays. With these promising results on the new polymeric substrates, future studies will be oriented toward the production of porous structures made from these materials to create an improved keratoprosthesis.

**Acknowledgment.** This work was supported by the Ministerio de Educación y Ciencia through the grant MAT2003-5391. A.C.F., J.L.G.R., J.M.M.D., and M.M.P. acknowledge the support of G.V.A. through the grant Grupos03/018. Authors acknowledge Drs. Diebold and Calonge, Institute for Applied Ophthalmology (IOBA) at Valladolid (Spain), for their kind donation of the IOBA-NHC cell line. Authors are also thankful to A. Arredondo and F. Granger for their help on sample preparation, water absorption, and contact angle measurements of some of the samples and to Dr. Dolores Ortiz for assistance with statistical analysis.

## References and Notes

(1) Hicks, C. R.; Fitton, J. H.; Chirila, T. V.; Crawford, G. J.; Constable, I. J. *Surv. Ophthalmol*. **1997**, *42*, 175−189.
(2) Minami, Y.; Sugihara, H.; Oono, S. *Invest. Ophthalmol. Vis. Sci*. **1993**, *34*, 2316−2324.
(3) Griffith, M.; Osborne, R.; Munger, R.; Xiong, X.; Doillon, C. J.; Laycock, N. L.; Hakim, M.; Song, Y.; Watsky, M. A. *Science* **1999**, *286*, 2169−2172.
(4) Germain, L.; Carrier, P.; Auger, F. A.; Salesse, C.; Guerin, S. L. *Prog. Retinal Eye Res.* **2000**, *19*, 497−527.
(5) Zorlutuna, P.; Tezcaner, A.; Kíyat I.; Aydínlí, A.; Hasírcí, V. *J. Biomed. Mater. Res.* **2006**, *79A*, 104−113.
(6) Evans, M. D. M.; Taylor, S.; Dalton, B. A.; Lohmann, D. *J. Biomed. Mater. Res.* **2003**, *64A*, 357−364.
(7) Sweeney, D. F.; Xie, R. Z.; O'Leary, D. J.; Vannas, A.; Odell, R.; Schindhelm, K.; Cheng, H. Y.; Steele J. G.; Holden B. A. *Invest. Ophthalmol. Vis. Sci*. **1998**, *39*, 284−291.
(8) Legeais, J. M.; Renard, G.; Parel, J. M.; Savoldelli, M.; Pouliquen, Y. *Arch. Ophthalmol*. **1995**, *113*, 757−763.
(9) Legeais, J. M.; Renard G. *J. Fr. Ophtalmol*. **1987**, *10*, 425−433.
(10) Legeais, J. M.; Rossi, C.; Renard, G.; Salvoldelli, M.; D'Hermies, F.; Pouliquen, Y. J. *Cornea* **1992**, *11*, 538−545.
(11) Legeais, J. M.; Renard, G.; Pouliquen, Y. *J. Fr. Ophtalmol*. **1993**, *16*, 577−583.
(12) Drubaix, I.; Legeais, J. M.; Malek-Chehire, N.; Savoldelli, M.; Ménasche, M.; Robert, L.; Renard, G.; Pouliquen, Y. *Exp. Eye Res*. **1996**, *62*, 367−376.
(13) Legeais, J. M.; Renard, G.; Parel, J.M.; Serdarevic, O.; Mei-Mui, M.; Pouliquen, Y. *Exp. Eye Res*. **1994**, *58*, 41−52.
(14) Chirila, T. V.; Constable, I. J.; Crawford, G. J.; Vijayasekaran, S.; Thompson, D. E.; Chen, Y. C.; Fletcher, W. A.; Griffin, B. J. *Biomaterials* **1993**, *14*, 26−38.
(15) Chirila, T. V.; Chen, Y. C.; Griffin, B. J.; Constable, I. J. *Polym. Int.* **1993**, *32*, 221−232.
(16) Clayton, A. B.; Chirila, T. V.; Dalton, P. D. *Polym. Int*. **1997**, *42*, 45−56.
(17) Vijayasekaran, S.; Fitton, J. H.; Hicks, C. R.; Chirila, T. V.; Crawford, G. J.; Constable, I. J. *Biomaterials* **1998**, *19*, 2255−2267.
(18) Ziegelaar, B. W.; Fitton, J. H.; Clayton, A. B.; Platten, S. T.; Maley, M. A. L.; Chirila, T. V. *Biomaterials* **1999**, *20*, 1979−1988.
(19) Trinkaus-Randall, V.; Capecchi, J.; Newton, A.; Vadasz, A; Leibowitz, H.; Franzblau, C. *Invest. Ophtalmol. Vis. Sci*. **1988**, *29*, 393−400.
(20) Trinkaus-Randall, V.; Capecchi, J.; Sammon, L.; Gibbons, D.; Leibowitz, H. M.; Franzblau, C. *Invest. Ophthalmol. Vis. Sci*. **1990**, *31*, 1321−1326.
(21) Trinkaus-Randall, V.; Banwatt, R.; Capecchi, J.; Leibowitz, H. M.; Franzblau, C. *Invest. Ophthalmol. Vis. Sci*. **1991**, *32*, 3245−3251.
(22) Tsuk, A. G.; Trinkaus-Randall, V.; Leibowitz, H. M. *J. Biomed. Mater. Res*. **1997**, *34*, 299−304.
(23) Trinkaus-Randall, V.; Wu, X. Y.; Tablante, R.; Tsuk, A. *Int. J. Artif. Organs* **1997**, *21*, 1185−1191.
(24) von Fischern, T.; Langefeld, S.; Yuan, L.; Volcker, N.; Reim, M.; Kirchhof, B.; Schrage, N. F. *Int. J. Artif. Organs* **1999**, *22*, 52−57.
(25) Crawford, G. J.; Hicks, C. R.; Lou, X.; Vijayasekaran, S.; Tan, D.; Mulholland, B.; Chirila, T. V.; Constable, I. J. *Ophthalmology* **2002**, *109*, 883−889.
(26) Latkany, R.; Tsuk, A.; Sheu, M. S.; Loh, I. H.; Trinkaus-Randall, V. R. *J. Biomed. Mater. Res*. **1997**, *36*, 29−37.
(27) Diebold, Y.; Calonge, M.; Enríquez de Salamanca, A; Callejo, S.; Corrales, R. M.; Saez, V.; Siemasko, K. F.; Stern, M. E. *Invest. Ophthalmol. Vis. Sci*. **2003**, *44*, 4263−4274.
(28) Perez Olmedilla, M.; Garcia-Giralt, N.; Monleón Pradas, M.; Ruiz, P. B.; Gómez Ribelles, J. L.; Cáceres Palou, E.; Monllau García, J. C. *Biomaterials* **2006**, *27*, 1003−1012.
(29) Soria, J. M.; Martínez-Ramos, C.; Benavent, V.; Campillo Fernández, A.; Gómez Ribelles, J. L.; Salmerón Sánchez, M.; García Verdugo, J. M.; Monleón Pradas, M.; Barcia, J. A. *J. Biomed. Mater. Res., Part A* **2006**, *79* (A), 495−502
(30) Soria, J. M.; Martínez Ramos, C.; Bahamonde, O.; Garcia Cruz, D. M.; Salmerón Sánchez, M.; Garcia Esparza, M. A.; Casas, C.; Guzmán, M.; Navarro, X.; Gómez Ribelles, J. L.; Garcia Verdugo, J. M.; Monleón Pradas, M.; Barcia, J. A. Influence of the substrate's hydrophilicity on the in vitro Schwann cells viability. *J. Biomed. Mater. Res. A* **2007**, May 3, Epub ahead of print.
(31) Owens, D. K.; Wendt, R. C. *J. Appl. Polym. Sci*. **1969**, *13*, 1741−1747.
(32) Tziampazis, E.; Kohn, J.; Moghe, P. V. *Biomaterials* **2000**, *21*, 511−520.
(33) Rodríguez Hernández, J. C.; Salmerón Sánchez, M.; Soria, J. M.; Gómez Ribelles, J. L.; Monleón Pradas, M. *Biophys. J.* **2007**, *93* (1), 202−207.
(34) Lydon, M. J. *Br. Polym. J*. **1986**, *18*, 22−27.
(35) Lydon, M. J.; Minett, T. W.; Tighe, B. J. *Biomaterials* **1985**, *6*, 396−402.
(36) Horbett, T. A.; Schway, M. B.; Ratner, B. D. *J. Colloid. Interface Sci*. **1985**, *104*, 28−39.
(37) Kiremitci, M.; Pulat, M.; Senvar, C.; Serbetci, A. I.; Piskin, E. *Clin. Mater*. **1990**, *6*, 227−237.

(38) Rosen, J. J.; Schway, M. B. *Polym. Sci. Technol*. **1980**, *12*, 667−686.
(39) Horbett, T. A.; Waldburger, J. J.; Ratner, B. D.; Hoffman, A.S. *J. Biomed. Mater. Res*. **1988**, *22*, 383−404.
(40) Schneider, G. B.; English, A.; Abraham, M.; Zaharias, R.; Stanford, C.; Keller, J. *Biomaterials* **2004**, *25*, 3023−3028.

BM0703012